International Journal of Biological Macromolecules xxx (xxxx) 1–9

Contents lists available at ScienceDirect

International Journal of Biological Macromolecules

journal homepage: www.elsevier.com/locate/ijbiomac

New opportunities for sustainable bioplastic development: Tailorable polymorphic and three-phase crystallization of stereocomplex polylactide by layered double hydroxide

Qi Chen [a, b], Rafael Auras [c], Milena Corredig [a, b], Jacob Judas Kain Kirkensgaard [d, e], Aref Mamakhel [f], Ilke Uysal-Unalan [a, b, *]

[a] Department of Food Science, Aarhus University, Agro Food Park 48, 8200 Aarhus N, Denmark
[b] CiFOOD – Center for Innovative Food Research, Aarhus University, Agro Food Park, 48, 8200 Aarhus N, Denmark
[c] School of Packaging, Michigan State University, East Lansing, MI 48824-1223, USA
[d] Department of Food Science, University of Copenhagen, 1958 Frederiksberg C, Denmark
[e] Niels Bohr Institute, University of Copenhagen, 2100 Copenhagen Ø, Denmark
[f] Department of Chemistry, Aarhus University, 8000 Aarhus C, Denmark

UNCORRECTED PROOF

ARTICLE INFO

Keywords:
2D nanoparticle
Polymer nanocomposites
RAF
Nucleation
Thermal fluctuation

ABSTRACT

Stereocomplexation between enantiomeric poly(L-lactide) (PLLA) and poly(D-lactide) (PDLA) is a promising sustainable approach and gaining momentum to overcome the shortcomings of polylactide (PLA) for its use as a replacement for fossil-based plastics. Filler addition in tailoring the crystallization of stereocomplex PLA (SC-PLA) attracts extensive attention; however, research has primarily focused on the heterogeneous nucleation effect of filler. The impact of filler on the chain behavior of SC-PLA during crystallization has not been exclusively discussed, and the rigid amorphous fraction (RAF) development remains unknown. In this study, the crystallization of PLLA/PDLA blends was modified by low loading of layered double hydroxide (LDH) (≤ 1 wt%) with the proposed local effect of such filler, and additional RAF development was incurred. In the early stage of crystallization, LDH facilitates the pairing of PLLA and PDLA and arrests the ordered SC pairs during the dynamic balance between the separation and pairing of racemic segments. This explains the severely suppressed *homochiral* (HC) crystallization, promoted SC crystallization, and additional RAF formation driven by the nucleation-induced chain ordering. This work, for the first time, highlights the role of LDH in creating SC-PLA with tailorable polymorphism and RAF, where the mechanism can be extended to other filler-type nucleator systems.

1. Introduction

Polylactide (PLA) is a biobased, industrially compostable aliphatic polyester derived from the renewable resource lactic acid. PLA is poised to grow and gain greater research and industrial interest as a great addition to the green circular bioeconomy by replacing fossil-based polymers with its renewability and lowest-environmental footprint [1]. However, the gas and water vapor barrier and thermo-mechanical properties of PLA are less effective compared to several fossil-based polymers, greatly limiting its applications in end-use industries. So, tailoring the crystallization behavior of PLA can advance its material properties, driving its market position towards a more durable and high-performance polymer. Due to the recent rise in demand for sustainable materials, stereocomplexation between enantiomers of PLA, first reported by Ikada in 1987, has gained increasing attention to expand PLA applications [2]. This is because the stereocomplex (SC) crystal empowers the stereocomplex PLA (SC-PLA) with outstanding thermal, mechanical, barrier performances, and hydrolysis stability compared to homochiral PLA (HC-PLA) [3–5]. However, controlling the semicrystalline microstructure by modulating the crystallization of SC-PLA is challenging. For instance, there is competing crystallization between the HC and SC, leading to polymorphic structure. A rigid amorphous fraction (RAF) also develops [6]. RAF contains incomplete decoupled amorphous chain segments adjacent to the immobilized crystalline fractions (CF) [6]. Holding different chain conformations and free volume, RAF has a significant influence on the hydrolysis, barrier, and thermomechanical properties [6–8]. However, the study of RAF development during the competing HC and SC crystallization in SC-PLA is

* Corresponding author at: Department of Food Science, Aarhus University, Agro Food Park 48, 8200 Aarhus N, Denmark.
E-mail address: iuu@food.au.dk (I. Uysal-Unalan).

https://doi.org/10.1016/j.ijbiomac.2022.09.205
Received 26 July 2022; Received in revised form 20 September 2022; Accepted 22 September 2022
0141-8130/© 20XX

Note: Low-resolution images were used to create this PDF. The original images will be used in the final composition.

still in its infancy. Therefore, it is essential to understand the mechanisms controlling the RAF development and the competing HC and SC crystallization on PLA to deliver its full potential in both technological and sustainable benefits.

Because of the superior properties arising from SC crystals compared to HC crystals, efforts have been done to selectively promote SC crystallization to exploit its advantages and improve cost-effectiveness [9,10]. Promoting SC crystallization can be achieved by manipulating processing, chain architecture, blending, and introducing nucleating agent, filler, and plasticizer compounds [9,11]. Filler addition is of particular interest due to its compatibility with conventional melt processing technologies and the extra functionalities provided by the fillers. However, so far, research has mainly focused on the heterogeneous nucleation effect of filler and explaining only the promotion of SC crystallization [12,13]; the suppressed HC crystallization is not yet fully understood despite the well-known HC nucleation effect of SC crystals [14]. In this work, the modified competing crystallization mechanism of SC-PLA nanocomposites was investigated by the addition of a 2D layered nanosheet, layered double hydroxide (LDH).

LDH has the chemical formula $[M_{1-x}^{2+}M_x^{3+}(OH)_2]^{x+} \bullet A_{x/n}^{n-} \bullet mH_2O$, where M^{2+} and M^{3+} are cationic metals, and A^{n-} is the exchangeable anion alongside water molecules between the brucite-like sheets. These anions in the interlayer provide opportunities for versatile use of green technologies to produce polymer-compatible LDHs [15], that have great potential in building sustainable LDH filled polymer composites. The performance and crystallization of PLLA/LDH have been studied by several groups, mainly at a broad range of LDH loadings [16]. Urayama et al. [17] reported the nucleation effect of a mixture of phosphoric ester-aluminum complex and LDH on the SC-PLA. Yet, the crystallization behavior of SC-PLA/LDH has not been exclusively studied, particularly at low LDH loading (≤1 wt%). Low LDH loaded PLA composites may optimize the economic and technological benefits of the system, while minimizing the degradation effects, which may be caused by high filler content [18]. This work reports, for the first time, the role of LDH in the competing crystallization and RAF development of a symmetric PLLA/PDLA system. So far, little knowledge is available for RAF development in the SC-PLA system when a filler is also present. The present work rationalizes the utilization of fillers to fine tune SC-PLA properties by controlling the polymorphic and RAF composition. This new knowledge will assist in the future development of sustainable SC-PLA nanocomposite materials by employing a versatile and green approach with a wide range of customizable features for numerous applications.

2. Experimental section

2.1. Materials

Commercial PLLA (trade name Luminy® L130 with M_w ca. 160 kg/mol, $_D$-lactide content <1 %) and PDLA pellets (trade name Luminy® D120 with M_w ca. 120 kg/mol, $_L$-lactide content <1 %) were purchased from TotalEnergies Corbion (Gorinchem, Netherlands). The LDH (trade name DHT-4A, $Mg_{4.3}Al_2(OH)_{12.6}CO_3{\cdot}mH_2O$), modified by fatty acid (<4 %), was kindly provided by Kisuma Chemicals (Veendam, Netherlands). Dichloromethane (DCM) was purchased from Sigma (Søborg, Denmark), and 1,1,1,3,3,3-hexafluoro-2-propanol (HFIP) was purchased from abcr GmbH (Karlsruhe, Germany).

2.2. Preparation of SC-PLA and SC-PLA/LDH films

The PLLA/PDLA/LDH blends were prepared by solvent casting. The same amount of PLLA and PDLA pellets were dissolved at 5 wt% in DCM under stirring at room temperature overnight. LDH powders (0.1–1 wt% of PLLA/PDLA) were then dispersed into the solution by a shear mixer (Ultra Turrax, IKA, Denmark) at 9000 rad/s for 2 min. Then, the solution was poured into a glass Petri dish at ambient condition overnight, followed by oven drying at 70 °C for 12 h to evaporate all solvent. The obtained films were named based on LDH content, "xLDH", where x denotes the weight percentage of LDH based on the solid weight of PLLA/PDLA.

2.3. Differential scanning calorimetry (DSC)

The crystallization behavior of the solvent-casted films was studied using differential scanning calorimetry (DSC) (Q2000, TA instruments, New Castle, USA) with an RCS 90 cooler under 50 mL/min nitrogen gas flow. Solvent-casted films (5.5 ± 0.5 mg) were weighed for all measurements. The samples were heated to 250 °C and held for 5 min to erase their thermal history. For the nonisothermal crystallization studies, it is followed by cooling to 30 °C at 10 °C/min, and subsequent heating was run from 30 to 250 °C at 10 °C/min. For isothermal crystallization studies, after removing thermal history, samples were fast cooled at approximately 60 °C/min to various temperatures (i.e., 90, 110, 130, and 140 °C) and measured isothermally until no more differential heat flow was detected because of crystallization; the crystallized samples were then cooled to 30 °C and reheated to 250 °C at 10 °C/min.

Modulated DSC (MDSC) (Q2000, TA instruments, New Castle, USA) was employed to study the three-phase crystalline composition of nanocomposites. The MDSC measurements were conducted with a modulation amplitude of ±0.318 °C, period of 60s, and heating rate of 2 °C/min. To investigate the impact of LDH on the three-phase crystalline composition before crystallization, solvent-casted films were heated to 250 °C for removing thermal history then fast cooled to 0 °C with 60 °C/min followed by the MDSC measurement to 100 °C. For studying the impact of crystallization on the three-phase crystalline composition, solvent-casted films after removing thermal history at 250 °C were fast cooled to 140 °C with 60 °C /min and held at 140 °C for different times by isothermal MDSC. Afterwards, the samples were further quenched to 0 °C with 60 °C/min followed by the MDSC measurement to 250 °C.

The crystalline fraction (CF), the rigid amorphous fraction (RAF), and the mobile amorphous fraction (MAF) of nanocomposites can be calculated by the following equations: [19,20]

$$CF = CF_{HC} + CF_{SC} = \frac{\Delta H_{HC} - \Delta H_{Cold}}{\Delta H_{HC}^{0}\left(1 - w_{LDH}\right)} + \frac{\Delta H_{SC}}{\Delta H_{SC}^{0}\left(1 - w_{LDH}\right)} \quad (1)$$

$$MAF = \frac{\Delta C_{p,composites}}{\Delta C_{p,amorphous}^{SC-PLA}\left(1 - w_{LDH}\right)} \quad (2)$$

$$RAF = 1 - CF - MAF \quad (3)$$

The CF_{HC} and CF_{SC} are the crystallinity of the HC and SC, respectively, determined by the ratio of measured (ΔH_{HC}, ΔH_{SC}) and theoretical melting enthalpy (ΔH_{HC}^0, ΔH_{SC}^0). Recent studies suggested that ΔH_{HC}^0 is temperature-dependent and related to the crystal form of PLA [6,21]. Herein, 143 J/g [21], 107 J/g [21], and 142 J/g [22] were chosen as the theoretical melting enthalpy of α, α′, and SC form of crystal, respectively. The w_{LDH} refers to the weight fraction of LDH. For a few samples, ΔH_{Cold} is the cold crystallization enthalpy. $\Delta C_{p,\ composites}$ is the measured heat capacity change at the glass transition temperature. $\Delta C_{p,\ amorphous}^{SC-PLA}$ equaling to 0.53 J/g K is the heat capacity change of amorphous SC-PLA at glass transition temperature after fast cooling the sample from 250 °C to 0 °C at 60 °C/min [19]. The value is similar to the measured values in other works for amorphous PLLA [23,24].

2.4. Wide angle X-ray analysis (WAXS)

WAXS was performed using a Nano-inXider (λ = 0.154 nm, Xenocs, Sassenage, France) operated at 50 kV, 0.6 mA, beam size 800 μm, and covering as q range from 0.37 to 4 $Å^{-1}$. To study the nucleation effect of

CORRECTED PROOF

LDH on the nanocomposites, WAXS of solvent-casted films after nonisothermal crystallization in DSC as described above were measured with an exposure time of 600 s. To study the time-resolved crystallization of partially melted nanocomposites, in-situ WAXS was performed. The solvent-casted films were placed in a heating plate (HFSX350, Linkam scientific instruments ltd., Surrey, United Kingdom) under a vacuum and heated from 30 °C to 260 °C at 30 °C/min and then immediately cooled to 30 °C at 10 °C/min.

3. Results and discussion

3.1. Competing crystallization behavior of nanocomposites

Nonisothermal crystallization of SC-PLA nanocomposites was studied by DSC. Fig. 1 shows the heat flow of nanocomposites with different LDH content during cooling from 250 °C to 30 °C (Fig. 1A) and subsequent heating (Fig. 1B) to 250 °C at 10 °C/min. Under these conditions, the nanocomposite films are thermally stable as measured by the TGA analysis up to 600 °C (Fig. S1). As shown in Fig. 1A, neat SC-PLA shows a small exothermal crystallization peak around 100 °C during cooling. Increasing LDH loading leads to a more pronounced crystallization peak while shifting it to a higher temperature. This indicates the heterogeneous nucleation of polymer crystallization where crystal grows onto a foreign surface, as widely observed in both PLA/LDH [25] and other PLA/filler systems [18]. The heterogeneous effect of LDH can be attributed to the favorable interaction between PLA and the filler surface with abundant hydroxyl groups [26].

During the subsequent heating after nonisothermal crystallization (Fig. 1B), neat SC-PLA exhibits two melting peaks. An intensive melting peak of HC crystals is around 175 °C, and a very low-intensity peak at 220 °C corresponds to the melting peak of SC crystals, as commonly seen in high molecular weight SC-PLA systems [27]. In contrast, after the introduction of 0.2 wt% LDH, the polymorphic crystallization was significantly modified. The SC crystallinity was enhanced with a more noticeable melting peak while HC crystallinity was drastically reduced with a negligible melting peak. When LDH content is further increased to 0.5 and 1 wt%, only the melting peaks of SC crystals are observed around 210 °C, while the melting peaks of HC crystals disappear completely. This demonstrates that during the nonisothermal crystallization (Fig. 1A), the heterogeneous nucleation effect of LDH is associated with SC crystallization. WAXS and FTIR analysis was also performed on the films after nonisothermal crystallization (Fig. 1C and D). The X-ray diffraction patterns clearly showed different crystal forms depending on the LDH content as denoted. In the neat SC-PLA after nonisothermal crystallization, there was only one peak around 17°, corresponding to the 110/200 diffraction planes of HC crystal [28], and the cooling rate may be too fast to initiate SC crystallization. However, in the LDH filled SC-PLA nanocomposites, the diffraction peaks corresponding to SC crystal appeared and increased with an increase in LDH content, demonstrating the selective nucleation effect of LDH on SC crystallization, which was also confirmed in the FTIR (Fig. 1D) curves by the increased absorption of paired $3_2/3_1$ helices in SC at 908 cm^{-1}. Fig. S2 shows the DSC heating curves of homochiral PLA (PLLA or PDLA) filled with LDH after the same nonisothermal crystallization procedure from

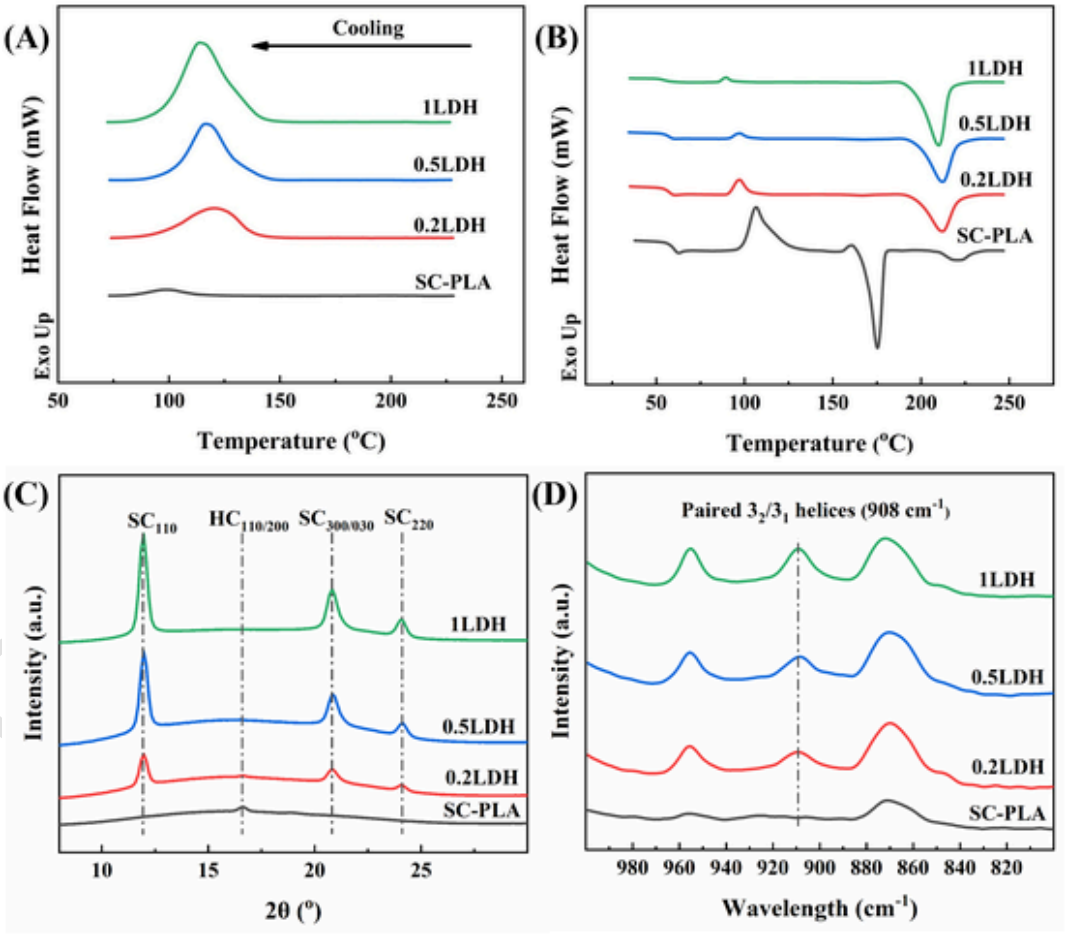

Fig. 1. Heat flow of SC-PLA nanocomposite films with various LDH content measured during (A) cooling from 250 °C to 30 °C at 10 °C/min and (B) subsequent heating to 250 °C at 10 °C/min, and corresponding X-ray diffraction (C) and FTIR spectra (D) of the nanocomposite after the nonisothermal crystallization cooling from 250 °C to 30 °C.

250 °C. The nucleation effect of LDH on crystallization was not observed with the unchanged crystallinity of PLLA and PDLA. This difference in heterogeneous nucleation effect on SC and HC crystallization demonstrates the nucleation selection process to match the lattice periodicity with the nucleating agent [29]. The underlying mechanism and influence of the nucleation selection of LDH on the crystallization of SC-PLA will be discussed in the following sections.

Isothermal crystallization of the nanocomposites was also studied. The heat flow during isothermal crystallization of the nanocomposites at 140 °C and 90 °C with various LDH content is shown in Fig. 2A and B, respectively. The exothermal peaks of crystallization were higher and shifted towards shorter times with increasing LDH content whereas that of neat SC-PLA is much broader and flatter. This implies the faster overall crystallization rates which were caused by the heterogeneous nucleation effect of LDH. Fig. S3 shows the subsequent heating of samples after quenching from isothermal crystallization temperatures. No cold crystallization peak was observed during the heating, indicating the crystallization was complete within the 30 min isothermal crystallization. Similar to the nonisothermal crystallization, the neat SC-PLA showed two endothermic peaks around 175 and 220 °C, corresponding to the melting of HC crystals and SC crystals, respectively. The nanocomposites with LDH content higher than 0.5 wt% only exhibited a melting endothermic peak around 210 °C. This confirms the selective nucleation effect of LDH on SC crystallization. The crystallization half time, expressed as $t_{1/2}$ (time required to reach 50 % of final crystallinity), and the crystallinity of nanocomposites after isothermal crystallization at various temperatures was summarized in Fig. S4. Compared to the 15 % of SC crystallinity and 9 min of $t_{1/2}$ in neat SC-PLA, the SC crystallinity in 0.5LDH doubled to 30 % and the $t_{1/2}$ decreased fourfold to ca. 2 min at the 140 °C of isothermal crystallization. The results demonstrate that LDH can be an efficient selective nucleating agent for SC crystallization, which might drive the use and application development of PLLA/PDLA/LDH nanocomposites.

Interestingly, at a very low concentration of LDH (0.1 wt%), the exothermal peak of crystallization was retarded when it was HC-dominated at both temperatures. This means that the HC crystallization is suppressed in presence of the demonstrated LDH-induced SC crystallization. It has been widely reported that SC crystals can facilitate HC crystallization [14,30,31]; however, suppressed HC crystallization by SC crystals was also observed [31,32]. This is attributed to the constrained chain mobility by the highly developed SC crystalline network [31,32], which may not the case with low content of SC crystals and fillers. Fig. 3 further demonstrates the suppressed HC crystallization by showing the in-situ WAXS patterns of partially melted neat SC-PLA and the 0.5LDH nanocomposites during cooling from 260 °C to 50 °C. In neat SC-PLA, HC crystallization developed quickly in the presence of SC crystals, which was attributed to the HC-nucleation effect of the SC crystal [33–35]. In contrast, the nanocomposites containing 0.5 wt%

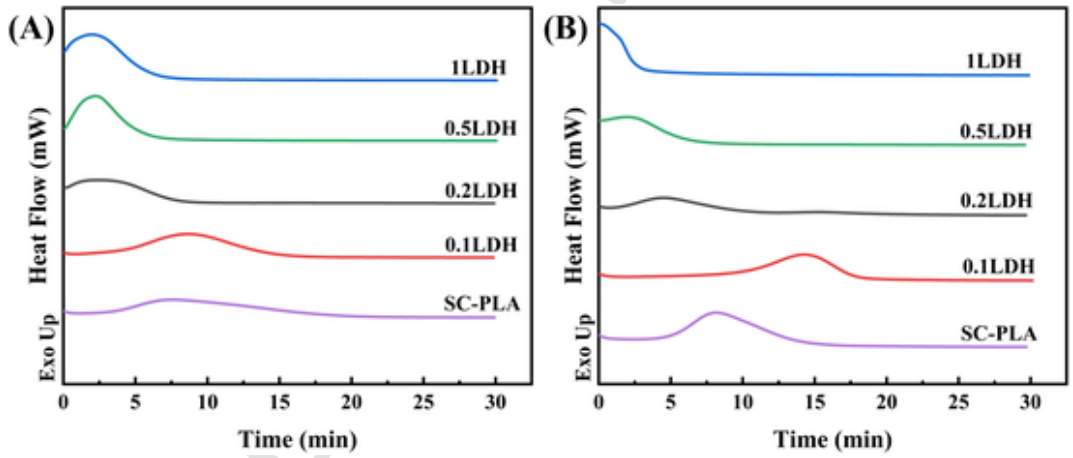

Fig. 2. Heat flow of SC-PLA nanocomposite films with various LDH content measured during isothermal crystallization at (A) 140 °C and (B) 90 °C for 30 min.

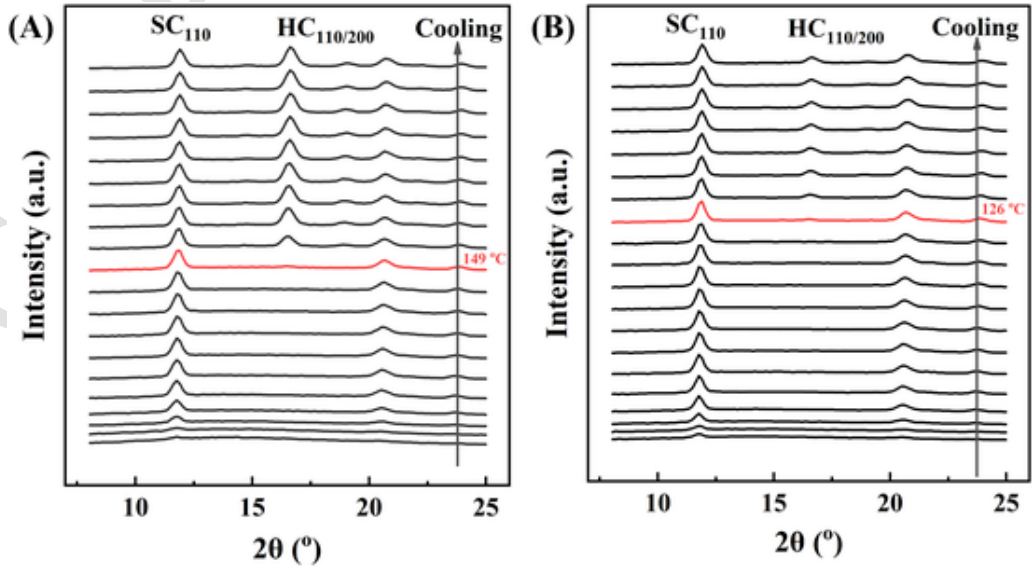

Fig. 3. In-situ WAXS intensity profiles of partially melted (A) SC-PLA and (B) 0.5LDH during cooling at 10 °C/min from 260 °C to 50 °C.

LDH showed suppressed HC crystallization with a low content of SC crystals, as also observed by DSC (Fig. S5). Therefore, the addition of LDH inhibits or counteracts the HC-nucleation capacity of the SC crystals. It is believed that nucleation involves the selection of chains from amorphous melt to match the crystal lattice [29]. Therefore, the nucleation selection induced by LDH suppresses the HC crystallization, possibly by inhibiting the HC-nucleation capacity of the existing SC crystals.

Recent research suggests the 'two-step' nucleation models for polymer crystallization to describe the details of polymer chains before nucleation or in the early stage of crystallization [36,37]. According to the models, amorphous melt would adopt low energy barrier intermediates as pathways before nucleation [36], as firstly conceptualized by the Ostwald stage rule for phase transition [29]. Instead of directly transforming into ordered and densified crystalline phases, as described in the classical nucleation model [36], the pre-ordering and densification of amorphous melt would happen in sequence [36,38]. Therefore, ordered and/or densified precursors are formed before nucleation. This has been demonstrated for PE [29,39] and PLLA [37]. For a polymorphic system, the model rationalizes that, prior to nucleation, a selection process occurs in the intermediate stage to determine a preferred crystal form driven by thermodynamics [40]. Yet, the development of the two-step model is still in place for polymer crystallization [29]; the evidence of existing precursors continues to be reported [29,36]. For SC-PLA, though the focus has not been on the two-step nucleation model, many authors have highlighted its heterogeneous melt behavior before nucleation [41,42]. Yang [42] reported the precursor formation of hydrogen bonding racemic helical pairs that transforms into the cluster ('mesophase') prior to the SC crystal formation. Subsequently, it has been widely observed that the presence of nucleating agents, fillers, or shear can boost the precursor formation, therefore showing promoted SC crystallization [13,26,43].

Fig. 4 proposes a mechanism of the competing polymorphic crystallization in SC-PLA. On one hand, separation of racemic segments may occur due to their thermodynamic immiscibility [44–46], or due to the kinetically favored HC crystallization [47]. On the other hand, at the same time, due to thermal fluctuation, the racemic segments can be paired by hydrogen bonding that leans towards SC nucleation [42,48]. Therefore, the crystallization is determined prior to nucleation by the dynamic balance between separation and SC pairing of racemic segments in the supercooled melt. Similarly, the idea of separation was proposed early in 1991 by Tsuji et al. [49], and in 2012 by Yang et al. [42], which work attempted to explain the nucleation of SC-PLA beyond the scope of the classical nucleation model. Recent works by Feng et al. [44,45] and Huang et al. [33] suggested a multiphase structure in PLLA/PDLA system comprised of homopolymer phases, and mixed PLLA/PDLA phases. These works support our proposed mechanism where both separation and intermolecular bonding of PLLA/PDLA can coexist in the melt prior to crystallization. For the role of filler, it may not directly improve the thermodynamic miscibility between the racemic segments as suggested in other promoted SC systems [46]. Instead, it arrests the paired racemic segments during the thermal fluctuations [12], suppressing the separation for HC crystallization and causing a favorable condition for SC crystallization in the supercooled melt. Moreover, as illustrated in Fig. 4, such effects might occur locally in the regions near fillers, so as in the 0.1LDH (Fig. 2), the overall isothermal crystallization is HC-dominated as the neat SC-PLA but suppressed. Further increase in the LDH content leads to the saturation of the affected regions, accounting for the drastic change in crystallization behavior.

LDH may induce the modified crystallization by contributions from multiple effects; further work is needed to understand the individual effects of structural factors of LDH, such as dimension, metal cations, and surface modifications. The surface morphologies of as-received LDH by TEM and AFM (Fig. S6) analysis and its chemical structure by XRD and FTIR (Fig. S7) were fully characterized and discussed in detail in the supplementary material. Briefly, the findings demonstrated typical LDH characteristics and confirmed its modification by fatty acidic surfactant. For further understanding of the proposed mechanism, we investigated the effect of the interlayer water on the competing crystallization. Fig. 5A shows the isothermal crystallization of SC-PLA affected by as-received LDH as compared with dried LDH where the interlayer water was removed by a TGA procedure as shown in Fig. S8A. With the increase of filler, the suppressed HC-dominated crystallization is further demonstrated in dried LDH, confirming the proposed mechanism with the accumulable local effect on crystallization. Fig. 5 indicated that dried LDH still acts as the selective SC nucleating agent, probably due to the remained hydroxyl group. Fig. S8B shows the chromatographs of SC-PLA nanocomposites after the isothermal crystallization at 140 °C. Although the nanocomposites are thermally stable in the present study (TGA, Fig. S1) as commonly claimed in other systems, it is normally neglected that PLA degradation can happen. However, significantly altered crystallization in slightly degraded 0.2LDH nanocomposites means that the LDH-induced degradation does not dictate the competing crystallization. This is also evidenced by the negligible effect of LDH on the crystallization of individual PLLA and PDLA [50] (Fig. S2) after the same thermal conditions are applied. Therefore, the difference between LDH and dried LDH may be attributed to the locally facilitated racemic pairing assisted by interlayer water through plasticization or compatibilization.

3.2. Three-phase crystalline structure of nanocomposites

During crystallization, the polymer chains present in the mobile amorphous fraction (MAF) can either be ordered into the crystalline

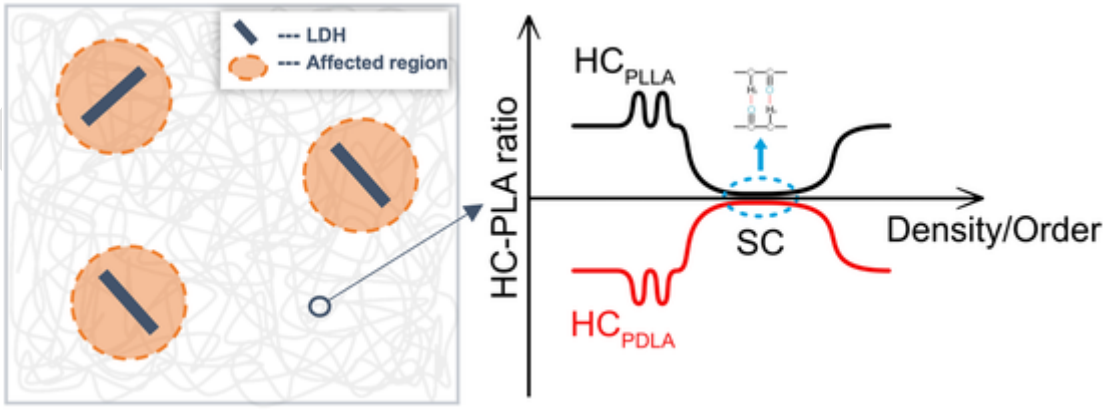

Fig. 4. Possible mechanism for the polymorphic crystallization in a filler-nucleated SC-PLA system controlled by dynamic balance between separation and pairing of racemic segments in thermal fluctuation. The balance can be significantly modified in the region near the filler, denoted as affected region.

CORRECTED PROOF

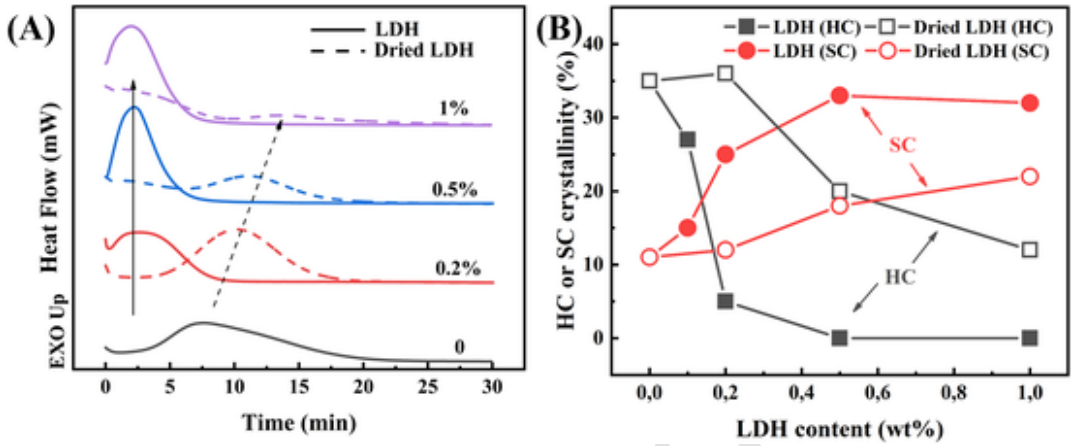

Fig. 5. (A) Heat flow of solvent-casted SC-PLA nanocomposites filled with LDH and dried LDH at different loadings (denoted by the percentages) during isothermal crystallization at 140 °C. The dash arrow shows the gradual retardation of HC crystallization induced by LDH, while the solid arrow shows the promotion of SC crystallization. (B) SC and HC crystallinity of SC-PLA nanocomposites after the 140 °C isothermal crystallization.

fraction (CF) or form rigid amorphous fractions (RAF). With polymer chains continuously attaching and detaching from the crystal growth front, the detached segments attempt to decouple from the CF, modifying their conformation and merging into the MAF as random coils [6]. However, decoupling of polymer segments is hindered by chain immobilization near the crystalline phase boundaries. The incomplete decoupled segments constitute the RAF regions; therefore, the development of RAF reflects the extent of constrained amorphous polymer segments with decreased mobility and fixed conformation [51]. The constrain also occurs in the polymer nanocomposite systems, such as, by the chain immobilization onto the nanofiller surface to form the filler-induced RAF (RAF_{filler}) [52].

The RAF can be estimated by the change of heat capacity (ΔC_p) at the glass transition temperature, where the ΔC_p is proportional to the extent of mobile segments participating in the glass transition [53,54]. Fig. 6A shows the heat capacity of nanocomposites with different LDH content and isothermal crystallization times. ΔC_p does not show obvious variations with different LDH content in quenched samples. In contrast, after holding nanocomposites for different crystallization times at 140 °C, there was a decrease in the ΔC_p, corresponding to the increasing number of segments from MAF that were immobilized in CF and RAF during crystallization. The difference demonstrates that LDH incurred negligible RAF_{filler} in the quenched nanocomposites, as also quantified by the relative variation of ΔC_p in Fig. 6B and observed in other work at low LDH content [19]. Fig. 6B also depicts that the glass transition temperature (T_g) drops with increasing LDH content. The drops can be attributed to either the plasticizer effect of the interlayer water, the loose packing of PLLA [23], or the spatial nanoconfinement of intercalated chains [55].

The evolution of MAF and CF during isothermal crystallization at 140 °C is plotted in Fig. 7A. Both MAF and CF changed drastically for SC-PLA after 5 min crystallization, whereas less for 0.5LDH, due to the short $t_{1/2}$. Fig. 7B summarizes the three-phase composition of the samples with different LDH content after crystallization at 140 °C for 60 min. Incorporation of just 0.2 wt% LDH showed a dramatic effect on the three-phase crystalline composition: there is a lower RAF, higher MAF, and corresponding lower CF compared to the neat SC-PLA nanocomposites. As already discussed in the isothermal crystallization study, the crystallization of SC-PLA is HC-dominated, whereas the 0.2LDH is SC-dominated. Therefore, the changes might indicate that SC crystallization develops lower RAF than HC crystallization. However, only a few works have addressed the influence of the polymorphic crystallization of SC-PLA on RAF development, and the findings from these works are conflicting. Sangroniz et al. [20] work observed a lower RAF development in SC-dominating crystallization. Conversely, a high RAF developed in exclusive SC crystallization is also observed in other work

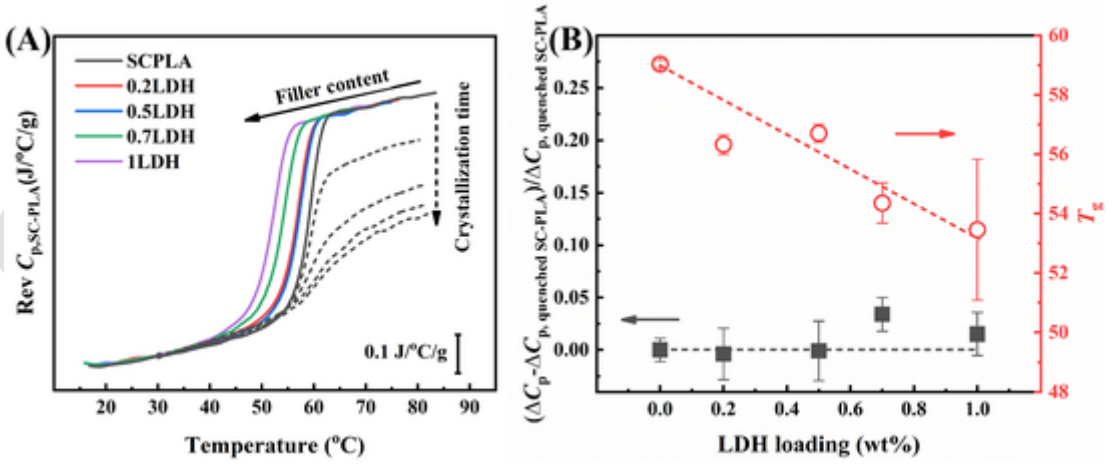

Fig. 6. (A) Reversible heat capacity of quenched SC-PLA nanocomposites with different LDH loadings (solid lines) and neat SC-PLA after different isothermal crystallization time at 140 °C (dash lines, 5, 10, 30, 60 mins from top down). The quenched samples were cooled from 250 °C to 0 °C at 60 °C/min. (B) The corresponding glass transition temperatures (T_g) and relative variation of heat capacity change (ΔC_p) at T_g for the quenched SC-PLA nanocomposites with different LDH content.

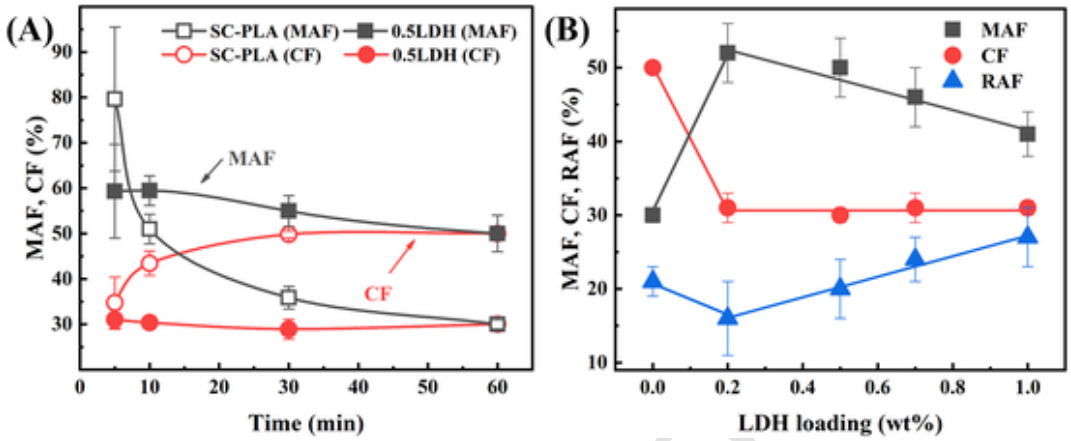

Fig. 7. (A) Evolution of MAF (black symbols) and CF (red symbols) of neat SC-PLA (hollow symbols) and 0.5LDH (solid symbols) after isothermal crystallization at 140 °C for different time. (B) Three-phase crystalline composition of SC-PLA nanocomposites with different LDH content after isothermal crystallization at 140 °C for 60 min. (For interpretation of the references to colour in this figure legend, the reader is referred to the web version of this article.)

[56]. And it was proposed by investigating a PLLA system that polymorphic crystallization does not influence RAF development [6]. Therefore, further work is needed to conclude the influence of HC and SC crystallization on RAF development in SC-PLA.

Notably, at LDH >0.2 wt% (Fig. 7B), CF remained constant with the increase of LDH, while there was a gradual decrease of MAF with LDH content. This corresponded to a mirroring increase of RAF and demonstrates the additional RAF formation incurred by LDH besides the crystallization induced RAF, as RAF was not developed in the quenched nanocomposites (Fig. 6). It is known that RAF is associated with conformational constraints of chains, such as incomplete decoupling from lamellas or adsorption on filler surface [6,24,53]. Therefore, such additional development of RAF may relate to the nucleation effect of LDH. This is to say, driven by the thermodynamic force in the supercooled melt, PLA chains are prone to attach to LDH for nucleation during thermal fluctuation. The attaching, within the frame of the proposed mechanism for the competing crystallization, might not always be followed by nucleation-into-crystallites. Instead, it can proceed with chain folding that induces the segments into the ordered conformation [57,58] near the location of LDH, rather than stays in a random coil conformation in MAF. The ordered conformation can lead to the increase of RAF during crystallization with increased LDH content. A similar filler-induced-ordering RAF development mechanism in PLA nanocomposites was also described elsewhere [23,59]. In the study of Klonos et al. [23] on the amorphous PLLA nanocomposites filled with 3D (silica and Ag), 2D (carbon nanotubes), and 1D nanoparticles (graphene oxide), the excessive RAF can be induced by filler by the 'pre-ordering' of polymer chains in amorphous status. In the present work, this was not seen in amorphous nanocomposites, instead, the 'pre-ordering' occurred in the supercooled melt, which is well consistent with the proposed mechanism herein where LDH facilitates the formation of SC paired helices as the stems attach onto crystal growth front via two-step nucleation. Consequently, the chain ordering facilitated by the heterogeneous nucleation in the early stage of crystallization leads to the formation of RAF in proximity to filler [12,60,61]. Although it is demonstrated in LDH filled SC-PLA, such mechanism can also be applied to the other filler-incorporated SC-PLA systems, which brings benefits in the optimization of the performance, such as hydrolysis, barrier, and mechanical properties.

4. Conclusion

The polymorphic and three-phase crystallization of green SC-PLA/LDH nanocomposites were studied with great promise to replace petroleum-based plastics. Adding a small quantity of LDH (≤1 wt%) can significantly modify the polymorphic HC and SC composition, and accelerate the kinetics of isothermal and non-isothermal crystallization, which grants a broad performance spectrum of the nanocomposites. More work is needed to elaborate on the impact of LDH on SC-PLA crystallization in terms of individual factors, such as surfactant, metal cations, interlayer ions, and dimension. The competition behavior between HC and SC crystallization was explained within the frame of the two-step nucleation model. Before nucleating into specific crystal nuclei, introducing LDH facilitates and arrests the paired PLLA/PDLA segments during the dynamic balance between the separation and pairing of racemic segments in the melt with the aid of interlayer water. This inhibits the HC crystallization and counteracts the HC-nucleation effect of existing SC crystals in the melt. Importantly, the modified chain behavior occurs locally around LDH and this renders the progressive retardation of HC-dominated crystallization with increasing LDH loading in the heterogeneous melt. The proposed mechanism is consistent with the additional RAF development in the nanocomposites. Under crystallization conditions, the supercooled melt favors the ordering of racemic PLA chains in proximity to LDH through its nucleating effect, leading to the ordered chain conformation that corresponds to the additional RAF development at the constant crystallinity. Owing to the greenery and versatility of production and the ability to control the crystallization of SC-PLA nanocomposites by filler-type nucleators, such renewable and biodegradable PLA stereocomplex-based composites open a broad application window with tailorable properties.

CRediT authorship contribution statement

Qi Chen: Conceptualization, Investigation, Methodology, Formal analysis, Validation, Visualization, Writing- Original draft preparation. **Rafael Auras**: Supervision, Writing - review & editing. **Jacob Judas Kain Kirkensgaard:** Investigation, Writing - review & editing. **Aref Mamakhel:** Investigation, Writing - review & editing. **Milena Corredig**: Supervision, Writing - review & editing. **Ilke Uysal-Unalan**: Conceptualization, Methodology, Funding acquisition, Supervision, Writing - review & editing.

Declaration of competing interest

The authors declare that they have no known competing financial interests or personal relationships that could have appeared to influence the work reported in this paper.

UNCORRECTED PROOF

Data availability

Data will be made available on request.

Acknowledgments

This work was supported by CiFOOD - Centre for Innovative Food Research in Aarhus University (AU). The authors would like to thank Laura Roman Rivas (Department of Food Science, AU) for her support with SEC-MALS, Bjarke Rolighed Jeppesen (iNano - Interdisciplinary Nanoscience Center, AU) for his support with AFM, and Mingdong Dong (iNano - Interdisciplinary Nanoscience Center, AU) and Zheshen Li (Department of Physics and Astronomy, AU) for offering access to FTIR. Data were generated through accessing research infrastructure at Aarhus University and University of Copenhagen, including FOODHAY (Food and Health Open Innovation Laboratory, Danish Roadmap for Research Infrastructure).

Appendix A. Supplementary data

Supplementary experimental methods; TEM images, AFM images, XRD patterns, and FTIR spectrums of LDH; Additional TGA, SEC, WAXD, and DSC results. Supplementary data to this article can be found online at https://doi.org/10.1016/j.ijbiomac.2022.09.205.

References

[1] Q. Chen, R. Auras, I. Uysal-Unalan, Role of stereocomplex in advancing mass transport and thermomechanical properties of polylactide, Green Chem. (2022).
[2] Y. Ikada, K. Jamshidi, H. Tsuji, S.H. Hyon, Stereocomplex formation between enantiomeric poly(lactides), Macromolecules 20 (4) (1987) 904–906.
[3] J.K. Muiruri, S. Liu, W.S. Teo, J. Kong, C. He, Highly biodegradable and tough polylactic acid-cellulose nanocrystal composite, ACS Sustain. Chem. Eng. 5 (5) (2017) 3929–3937.
[4] Z. Li, J.K. Muiruri, W. Thitsartarn, X. Zhang, B.H. Tan, C. He, Biodegradable silica rubber core-shell nanoparticles and their stereocomplex for efficient PLA toughening, Compos. Sci. Technol. 159 (2018) 11–17.
[5] Z. Li, B.H. Tan, T. Lin, C. He, Recent advances in stereocomplexation of enantiomeric PLA-based copolymers and applications, Prog. Polym. Sci. 62 (2016) 22–72.
[6] M.L. Di Lorenzo, M.C. Righetti, Crystallization-induced formation of rigid amorphous fraction, Polym. Cryst. 1 (2) (2018) e10023.
[7] J.H. Lee, S.H. Mahmood, J.-M. Pin, R. Li, P.C. Lee, C.B. Park, Determination of CO2 solubility in semi-crystalline polylactic acid with consideration of rigid amorphous fraction, Int. J. Biol. Macromol. 204 (2022) 274–283.
[8] X. Zhao, J. Liu, J. Li, X. Liang, W. Zhou, S. Peng, Strategies and techniques for improving heat resistance and mechanical performances of poly(lactic acid) (PLA) biodegradable materials, Int. J. Biol. Macromol. 218 (2022) 115–134.
[9] B.H. Tan, J.K. Muiruri, Z.B. Li, C.B. He, Recent Progress in using stereocomplexation for enhancement of thermal and mechanical property of polylactide, ACS Sustain. Chem. Eng. 4 (10) (2016) 5370–5391.
[10] A.V. Tuccitto, A. Anstey, N.D. Sansone, C.B. Park, P.C. Lee, Controlling stereocomplex crystal morphology in poly(lactide) through chain alignment, Int. J. Biol. Macromol. 218 (2022) 22–32.
[11] H. Chai, Y. Chang, Y. Zhang, Z. Chen, Y. Zhong, L. Zhang, X. Sui, H. Xu, Z. Mao, The fabrication of polylactide/cellulose nanocomposites with enhanced crystallization and mechanical properties, Int. J. Biol. Macromol. 155 (2020) 1578–1588.
[12] Z.Z. Gu, Y. Xu, Q.Q. Lu, C.J. Han, R.J. Liu, Z.P. Zhou, T.F. Hao, Y.J. Nie, Stereocomplex formation in mixed polymers filled with two-dimensional nanofillers, Phys. Chem. Chem. Phys. 21 (12) (2019) 6443–6452.
[13] H.L. Liu, W. Zhou, P.F. Chen, D.Y. Bai, Y.H. Cai, J.Y. Chen, A novel aryl hydrazide nucleator to effectively promote stereocomplex crystallization in high-molecular-weight poly(L-lactide)/poly (D-lactide) blends, Polymer 210 (2020).
[14] B. Wang, T. Wen, X. Zhang, A. Tercjak, X. Dong, A.J. Müller, D. Wang, D. Cavallo, Nucleation of Poly(lactide) on the surface of different fibers, Macromolecules 52 (16) (2019) 6274–6284.
[15] X. Wang, E.N. Kalali, D.-Y. Wang, Renewable cardanol-based surfactant modified layered double hydroxide as a flame retardant for epoxy resin, ACS Sustain. Chem. Eng. 3 (12) (2015) 3281–3290.
[16] J. Leng, P. Szymoniak, N.-J. Kang, D.-Y. Wang, A. Wurm, C. Schick, A. Schönhals, Influence of interfaces on the crystallization behavior and the rigid amorphous phase of poly(l-lactide)-based nanocomposites with different layered doubled hydroxides as nanofiller, Polymer 184 (2019) 121929.
[17] H. Urayama, T. Kanamori, K. Fukushima, Y. Kimura, Controlled crystal nucleation in the melt-crystallization of poly(l-lactide) and poly(l-lactide)/poly(d-lactide) stereocomplex, Polymer 44 (19) (2003) 5635–5641.
[18] R. Neppalli, V. Causin, C. Marega, M. Modesti, R. Adhikari, S. Scholtyssek, S.S. Ray, A. Marigo, The effect of different clays on the structure, morphology and degradation behavior of poly(lactic acid), Appl. Clay Sci. 87 (2014) 278–284.
[19] J. Leng, N. Kang, D.-Y. Wang, A. Wurm, C. Schick, A. Schönhals, Crystallization behavior of nanocomposites based on poly(l-lactide) and MgAl layered double hydroxides – unbiased determination of the rigid amorphous phases due to the crystals and the nanofiller, Polymer 108 (2017) 257–264.
[20] A. Sangroniz, A. Chaos, M. Iriarte, J. del Río, J.-R. Sarasua, A. Etxeberria, Influence of the rigid amorphous fraction and crystallinity on polylactide transport properties, Macromolecules 51 (11) (2018) 3923–3931.
[21] M.C. Righetti, M. Gazzano, M.L. Di Lorenzo, R. Androsch, Enthalpy of melting of α′- and α-crystals of poly(l-lactic acid), Eur. Polym. J. 70 (2015) 215–220.
[22] H. Tsuji, F. Horii, M. Nakagawa, Y. Ikada, H. Odani, R. Kitamaru, Stereocomplex formation between enantiomeric poly(lactic acid)s. 7. Phase structure of the stereocomplex crystallized from a dilute acetonitrile solution as studied by high-resolution solid-state carbon-13 NMR spectroscopy, Macromolecules 25 (16) (1992) 4114–4118.
[23] P. Klonos, Z. Terzopoulou, S. Koutsoumpis, S. Zidropoulos, S. Kripotou, G.Z. Papageorgiou, D.N. Bikiaris, A. Kyritsis, P. Pissis, Rigid amorphous fraction and segmental dynamics in nanocomposites based on poly(l–lactic acid) and nano-inclusions of 1–3D geometry studied by thermal and dielectric techniques, Eur. Polym. J. 82 (2016) 16–34.
[24] S.F. Nassar, A. Guinault, N. Delpouve, V. Divry, V. Ducruet, C. Sollogoub, S. Domenek, Multi-scale analysis of the impact of polylactide morphology on gas barrier properties, Polymer 108 (2017) 163–172.
[25] N. Delpouve, A. Saiter-Fourcin, S. Coiai, F. Cicogna, R. Spiniello, W. Oberhauser, S. Legnaioli, R. Ishak, E. Passaglia, Effects of organo-LDH dispersion on thermal stability, crystallinity and mechanical features of PLA, Polymer 208 (2020) 122952.
[26] Q. Xie, L.L. Han, G.R. Shan, Y.Z. Bao, P.J. Pan, Polymorphic crystalline structure and crystal morphology of enantiomeric poly(lactic acid) blends tailored by a self-assemblable aryl amide nucleator, ACS Sustain. Chem. Eng. 4 (5) (2016) 2680–2688.
[27] H. Tsuji, Y. Ikada, Stereocomplex formation between enantiomeric poly(lactic acids). 9. Stereocomplexation from the melt, Macromolecules 26 (25) (1993) 6918–6926.
[28] S. Lee, M. Kimoto, M. Tanaka, H. Tsuji, T. Nishino, Crystal modulus of poly (lactic acid)s, and their stereocomplex, Polymer 138 (2018) 124–131.
[29] B. Lotz, T. Miyoshi, S.Z.D. Cheng, 50th anniversary perspective: polymer crystals and crystallization: personal journeys in a challenging research field, Macromolecules 50 (16) (2017) 5995–6025.
[30] T. Wen, Z. Xiong, G. Liu, X. Zhang, S. de Vos, R. Wang, C.A.P. Joziasse, F. Wang, D. Wang, The inexistence of epitaxial relationship between stereocomplex and α crystal of poly(lactic acid): direct experimental evidence, Polymer 54 (7) (2013) 1923–1929.
[31] X.-F. Wei, R.-Y. Bao, Z.-Q. Cao, W. Yang, B.-H. Xie, M.-B. Yang, Stereocomplex crystallite network in asymmetric PLLA/PDLA blends: formation, structure, and confining effect on the crystallization rate of homocrystallites, Macromolecules 47 (4) (2014) 1439–1448.
[32] Q. Xie, J. Bao, G. Shan, Y. Bao, P. Pan, Fractional crystallization kinetics and formation of metastable β-form homocrystals in poly(l-lactic acid)/poly(d-lactic acid) racemic blends induced by precedingly formed stereocomplexes, Macromolecules 52 (12) (2019) 4655–4665.
[33] Y.-F. Huang, Z.-C. Zhang, Y. Li, J.-Z. Xu, L. Xu, Z. Yan, G.-J. Zhong, Z.-M. Li, The role of melt memory and template effect in complete stereocomplex crystallization and phase morphology of polylactides, Cryst. Growth Des. 18 (3) (2018) 1613–1621.
[34] P. Pan, L. Han, J. Bao, Q. Xie, G. Shan, Y. Bao, Competitive stereocomplexation, homocrystallization, and polymorphic crystalline transition in poly(l-lactic acid)/poly(d-lactic acid) racemic blends: molecular weight effects, J. Phys. Chem. B 119 (21) (2015) 6462–6470.
[35] Q. Xie, X.H. Chang, Q. Qian, P.J. Pan, C.Y. Li, Structure and morphology of Poly (lactic acid) stereocomplex nanofiber shish kebabs, ACS Macro Lett. 9 (1) (2020) 103–107.
[36] X.L. Tang, W. Chen, L.B. Li, The tough journey of polymer crystallization: battling with chain flexibility and connectivity, Macromolecules 52 (10) (2019) 3575–3591.
[37] J. Liu, C. Wang, Y. Chen, Q. Lan, Multistep nucleation mechanism of poly(l-lactide) revealed by nanocrystallization in low-pressure carbon dioxide, ACS Applied Polymer Materials (2022).
[38] X.L. Tang, J.S. Yang, T.Y. Xu, F.C. Tian, C. Xie, L.B. Li, Local structure order assisted two-step crystal nucleation in polyethylene, Phys. Rev. Mater. 1 (7) (2017).
[39] S.T. Milner, Polymer crystal-melt interfaces and nucleation in polyethylene, Soft Matter 7 (6) (2011) 2909–2917.
[40] M. Li, Y. Chen, H. Tanaka, P. Tan, Revealing roles of competing local structural orderings in crystallization of polymorphic systems, science, Advances 6 (27) (2020) eaaw8938.
[41] T. Lv, C. Zhou, J. Li, S. Huang, H. Wen, Y. Meng, S. Jiang, New insight into the mechanism of enhanced crystallization of PLA in PLLA/PDLA mixture, J. Appl. Polym. Sci. 135 (2) (2018) 45663.
[42] C.-F. Yang, Y.-F. Huang, J. Ruan, A.-C. Su, Extensive development of precursory helical pairs prior to formation of stereocomplex crystals in racemic polylactide melt mixture, Macromolecules 45 (2) (2012) 872–878.
[43] S. Yang, G.J. Zhong, J.Z. Xu, Z.M. Li, Preferential formation of stereocomplex in high-molecular-weight polylactic acid racemic blend induced by carbon nanotubes, Polymer 105 (2016) 167–171.
[44] L. Feng, X. Bian, G. Li, X. Chen, Compatibility and thermal and structural

CORRECTED PROOF

properties of poly(l-lactide)/poly(l-co-d-lactide) blends, Macromolecules (2022).
[45] L. Feng, X. Bian, G. Li, X. Chen, Thermal properties and structural evolution of poly(l-lactide)/poly(d-lactide) blends, Macromolecules 54 (21) (2021) 10163–10176.
[46] J. Liu, X. Qi, Q. Feng, Q. Lan, Suppression of phase separation for exclusive stereocomplex crystallization of a high-molecular-weight racemic poly(l-lactide)/poly(d-lactide) blend from the glassy state, Macromolecules 53 (9) (2020) 3493–3503.
[47] R. Zhang, L. Zha, W. Hu, Intramolecular crystal nucleation favored by polymer crystallization: Monte Carlo simulation evidence, J. Phys. Chem. B 120 (27) (2016) 6754–6760.
[48] K. Henmi, H. Sato, G. Matsuba, H. Tsuji, K. Nishida, T. Kanaya, K. Toyohara, A. Oda, K. Endou, Isothermal crystallization process of poly(L-lactic acid)/poly(D-lactic acid) blends after rapid cooling from the melt, ACS Omega 1 (3) (2016) 476–482.
[49] H. Tsuji, S.H. Hyon, Y. Ikada, Stereocomplex formation between enantiomeric poly(lactic acid)s. 4. Differential scanning calorimetric studies on precipitates from mixed solutions of poly(D-lactic acid) and poly(L-lactic acid), Macromolecules 24 (20) (1991) 5657–5662.
[50] S. Saeidlou, M.A. Huneault, H.B. Li, C.B. Park, Poly(lactic acid) crystallization, Prog. Polym. Sci. 37 (12) (2012) 1657–1677.
[51] J. del Río, A. Etxeberria, N. López-Rodríguez, E. Lizundia, J.R. Sarasua, A PALS contribution to the supramolecular structure of poly(l-lactide), Macromolecules 43 (10) (2010) 4698–4707.
[52] N. Jouault, J.F. Moll, D. Meng, K. Windsor, S. Ramcharan, C. Kearney, S.K. Kumar, Bound polymer layer in nanocomposites, ACS Macro Lett. 2 (5) (2013) 371–374.
[53] Z. Zheng, Y. Song, R. Yang, Q. Zheng, Direct evidence for percolation of immobilized polymer layer around nanoparticles accounting for sol-gel transition in Fumed silica dispersions, Langmuir 31 (50) (2015) 13478–13487.
[54] Q. Zia, D. Mileva, R. Androsch, Rigid amorphous fraction in isotactic polypropylene, Macromolecules 41 (21) (2008) 8095–8102.
[55] P.A. Klonos, L. Papadopoulos, Z. Terzopoulou, G.Z. Papageorgiou, A. Kyritsis, D.N. Bikiaris, Molecular dynamics in nanocomposites based on renewable poly (butylene 2,5-furan-dicarboxylate) in situ reinforced by montmorillonite nanoclays: effects of clay modification, crystallization, and hydration, J. Phys. Chem. B 124 (33) (2020) 7306–7317.
[56] N. Varol, Advanced Thermal Analysis and Transport Properties of Stereocomplex Polylactide, in: Normandie Université, 2019.
[57] W. Hu, T. Cai, Regime transitions of polymer crystal growth rates: molecular simulations and interpretation beyond Lauritzen-Hoffman model, Macromolecules 41 (6) (2008) 2049–2061.
[58] S. Yuan, Z. Li, Y.-L. Hong, Y. Ke, J. Kang, A. Kamimura, A. Otsubo, T. Miyoshi, Folding of polymer chains in the early stage of crystallization, ACS Macro Lett. 4 (12) (2015) 1382–1385.
[59] P.A. Klonos, L. Papadopoulos, G.Z. Papageorgiou, A. Kyritsis, P. Pissis, D.N. Bikiaris, Interfacial interactions, crystallization, and molecular dynamics of renewable Poly(Propylene Furanoate) in situ filled with initial and surface functionalized carbon nanotubes and graphene oxide, J. Phys. Chem. C 124 (18) (2020) 10220–10234.
[60] A. Wurm, M. Ismail, B. Kretzschmar, D. Pospiech, C. Schick, Retarded crystallization in Polyamide/Layered silicates nanocomposites caused by an immobilized interphase, Macromolecules 43 (3) (2010) 1480–1487.
[61] Y.-F. Mo, C.-L. Yang, Y.-F. Xing, M.-S. Wang, X.-G. Ma, L.-Z. Wang, Effects of silica surface on the ordered orientation of polyethylene: a molecular dynamics study, Appl. Surf. Sci. 311 (2014) 273–278.

CORRECTED PROOF